Photomechanical Surface Patterning in Azo-Polymer Materials

Kevin G. Yager* and Christopher J. Barrett*

Department of Chemistry, McGill University, Montreal, QC, Canada H3A 2K6

Received July 31, 2006; Revised Manuscript Received October 19, 2006

ABSTRACT: Azobenzene thin films undergo an unexplained spontaneous surface patterning when exposed to light intensity and/or polarization gradients. The elastic modulus of an azobenzene−polymer film is measured before and during laser irradiation using AFM indentation experiments. It is found that there is no significant change in elastic modulus with laser illumination, indicating that photosoftening can be neglected in these systems. In particular, this eliminates mechanisms that require photosoftening as candidate explanations for azo surface patterning. AFM measurements of patterning in azo-polymer thin films, irradiated at various temperatures, are compared to recent neutron reflectometry measurements of photomechanical effects in the same material. The magnitude and sign of the patterning exactly match the literature trend for photomechanical effects. This represents the first report of measuring both photoexpanded and photocontracted surface patterns in the same material, at different temperatures. These results are interpreted to mean that the unexplained surface mass transport phenomenon observed in the azobenzene system is in fact due to this newly identified photomechanical effect. Previous patterning results are discussed in terms of this explanation, and it is shown that the photomechanical effect can explain the vast majority of the literature results to date.

Introduction

Azobenzene chromophores exhibit a wide variety of photophysical and photoswitching effects.[1,2] The azo unit undergoes an efficient photoinduced isomerization between its trans and cis geometric isomers. This clean photochemistry gives rise to a variety of unique photoswitching and photomechanical effects. For instance, the material can be photooriented with polarized light (which induces birefringence), or thin films can be induced to macroscopically bend or unbend[3] (which has also been used to generate macroscopic locomotion[4]). The azobenzene unit is typically incorporated into a polymer system, whether amorphous or liquid crystalline, to improve processability and photophysical stability. In 1995, a remarkable effect was discovered in the azo-polymer materials.[5,6] Specifically, when the material was irradiated with two coherent laser beams (which generate a sinusoidally varying light pattern at the sample surface), the materials spontaneously deformed so as to generate a sinusoidal surface relief grating (SRG). An AFM image of a typical SRG is shown in Figure 1. This single-step all-optical surface patterning was found to be reversible, as the original film thickness could be recovered upon heating the material past its glass-to-rubber transition temperature (T_g). Thus, the process represents polymer motion over length scales of hundreds of nanometers, occurring readily at temperatures well below T_g. The facile patterning is a general phenomenon, with any incident light intensity and/or polarization pattern converted into a topography pattern. Various mechanisms have been proposed to explain the effect, although each has certain shortcomings. Thermal mechanisms have been discounted based on modeling of the temperature gradient during irradiation.[7] Gradient electric force mechanisms[8] naturally include the polarization dependence, but the predicted force density is too small.[9] An asymmetric diffusion model[10,11] was formulated but would seem to imply that the process would be most efficient for small-molecule materials, whereas in practice relatively high molecular weight polymers can be photopatterned. A mean-field model[12,13] predicts the correct phase behavior for liquid-crystalline systems, but not for amorphous polymers. A proposed isomerization pressure model[14,15] does not naturally include the polarization dependence of the patterning. A fundamental shortcoming of all presented explanations is that they cannot account for the phase relationship between the incident light field and the resultant patterning. In particular, all the models presented to date predict one phase relationship or the other (either material accumulates in the illuminated regions or in the dark regions), whereas experimentally both are observed in different systems. As a general rule, amorphous systems exhibit a "common" phase relationship (material accumulates in the dark regions of an incident light pattern) whereas the liquid crystalline azo systems exhibit an "inverted" phase relationship (material accumulation in the illuminated regions).[16] Some mechanisms imply that a form of photosoftening must be occurring during laser irradiation, in order to explain the material motion well below the glass-transition temperature. For instance, viscoelastic modeling assumed that the modulus decreased by 3 orders of magnitude during irradiation.[9] Thus, despite active research, the fundamental nature of the driving force remains unresolved.[17]

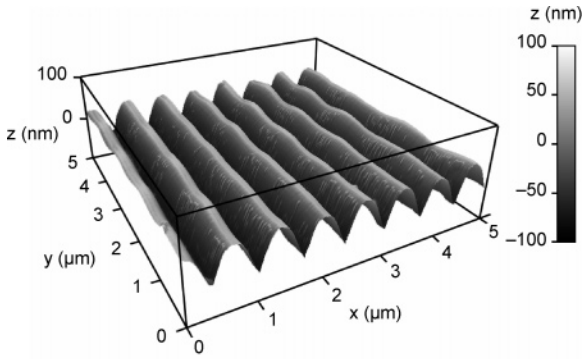

Figure 1. Atomic force micrograph of a surface relief grating (SRG) inscribed on an azo-polymer film by irradiating with a sinuisoidal light pattern.

Recently, photoexpansion in thin films of azo-polymer was measured using ellipsometry.[18] The material was found to

* E-mail: kevin.yager@mail.mcgill.ca and chris.barrett@mcgill.ca.

10.1021/ma061733s CCC: $33.50
Published on Web 12/01/2006

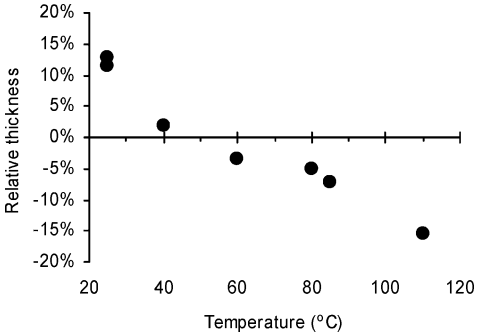

Figure 2. Relative film thickness (expansion or contraction) for thin azo films after irradiation with homogeneous laser light, as measured using neutron reflectometry. Below a crossover temperature (~50 °C for this material) the film photoexpands, whereas above the crossover, samples photocontract instead.

expand during laser illumination, with a large irreversible component that persists after illumination ceases and a smaller reversible component that exists only while the irradiating beam is active. This photomechanical effect was found to be directly related to the isomerization of the azo chromophores. A subsequent neutron reflectometry study analyzed this effect in more detail.[19] In addition to unambiguously confirming the photoexpansion of azo materials during light irradiation at room temperature, it was discovered that at elevated temperatures (above a distinct crossover at ~50 °C) the material instead contracted and became more dense when irradiated with laser light. The trend of this photomechanical effect (changing from expansion at low temperature to contraction at high temperature) is shown in Figure 2 and suggests a competition between two driving forces. At low temperature, the free volume requirement of the azobenzene isomerization induces a pressure on the polymer matrix and a subsequent expansion of the material. At these low temperatures, the polymer matrix cannot relax and the modification is persistent. Above the crossover temperature, however, the combination of photoinduced motion and thermally enabled motion is sufficient to allow the azo chromophores to migrate, aggregate, and eventually crystallize into higher-density states.

In this paper, we describe AFM measurements of the elastic modulus of azo materials before and during laser irradiation. These measurements indicate that photosoftening effects are quite small, which establishes a constraint on mechanisms proposed to explain surface mass patterning. We propose here that the photomechanical effect observed during homogeneous irradiation of azo films is the fundamental driving force for mass transport observed when the same materials are irradiated with light gradients. In order to critically test this theory, we conducted photopatterning experiments through a transmission mask, at various sample temperatures. The trend of the photopatterning, including both amplitude and sign, precisely matches the photomechanical trend. Moreover, the proposed patterning mechanism, with the exclusion of photosoftening, can be used to explain a variety of results in the azo-patterning literature, which previously appeared contradictory.

Experimental Methods

Sample Preparation. The azo-polymer material, poly[4′-[[2-(acryloyloxy)ethyl]ethylamino]-4-nitroazobenzene], often referred to as poly(disperse red 1 acrylate) (hereafter pdr1a), was synthesized as previously reported.[20] The prepared material was determined to have a molecular weight of 3700 g/mol, and a corresponding T_g in the range 95−97 °C. Samples for patterning were prepared by spin-coating the azo-polymer solutions (pdr1a in anhydrous THF solvent) onto cleaned glass microscope slides. The spin-coater acceleration was 1260 rpm/s, with a final velocity of 1300 rpm maintained for 35 s. Thin films were annealed in a vacuum oven at 110 °C for 8 h to remove any residual solvent or flow-induced orientation. Film thickness was measured by imaging a scratch in the thin film by AFM.

AFM Modulus Measurements. The elastic modulus of azo-polymer films was measured using AFM in force−distance mode (Nanoscope 3A, Digital Instruments) and applying a data analysis method already described in the literature.[21,22] Measurements were performed in a fluid cell (filled with ultrapure water) at room temperature in order to reduce adhesion artifacts. Measurements were performed before and during irradiation from a 532 nm diode laser. The laser light was coupled into the glass substrate that the thin film was cast onto. Internal reflections inside the glass substrate allowed the light to exit the film and irradiate the probed area. Successful irradiation of the probed region was confirmed visually and by irradiating for a long period of time, after which significant photopatterning was observed in the vicinity of the AFM tip. The AFM cantilevers were SiN probes with nominal tip radius 20−60 nm and a nominal spring constant of 0.12 N/m (NP probes, Digital Instruments). All the data reported in this paper were acquired using a single probe, thereby eliminating variability in the tip radius or spring constant. Although the inherent assumptions of tip geometry and spring constant introduce an uncertainty into the reported modulus values, using a single tip enables us to draw robust relative conclusions. The indentation rate was 0.2 Hz, and the indentation depth (<30 nm) was always considerably smaller than the film thickness (~200 nm). A large number of force indentation curves were recovered and analyzed using automated fitting software. Only those curves free of adhesion or other artifacts were automatically selected for further analysis. The final modulus values thereby obtained are spread across a certain range, owing to differences in the various indentation curves. A histogram of the results is thus used to analyze the statistical behavior. Each force curve is analyzed by extrapolating the linear noncontact region and the linear "infinitely stiff" region so as to identify the nonlinear elastic response region. This transition from the linear noncontact region to the nonlinear elastic response region is taken as the initial contact point. By assuming the AFM tip can be modeled as a sphere, the nonlinear region is fit to a force−distance equation of the form

$$F_{\text{sphere}} = \frac{4E\sqrt{R}}{3(1-\sigma^2)}\delta^{3/2} \tag{1}$$

where F is the measured force as a function of sample indentation δ, σ is the Poisson ratio for the material (taken to be 0.5, typical for polymers), R is the nominal tip radius, and E is the elastic modulus to be determined. Note that modeling the tip as a cone instead of a sphere provides a slightly different equation and thus modulus estimate. A cone model does not reproduce the data as faithfully as the selected sphere model but in any case would not alter the relative conclusion being drawn from the force−distance data in this paper.

Neutron Reflectometry. The neutron reflectometry measurements are described in detail in another publication.[19] The samples were held in a custom-built cell that enables neutron measurements simultaneous with optical irradiation.[23] The cell further allows control of sample environment, including ambient atmosphere and temperature. The presented photomechanical data were obtained for thin films maintained at various temperatures, under vacuum, and are based on comparison of the reflectivity curves before and after irradiation at those temperatures.

Transmission Mask Patterning. A single film of pdr1a (330 nm thick) was cut into small segments for the patterning experiment. The sample was placed inside a heating stage with optical windows on the front and back (INSTEC HCS302), driven by a temperature controller (INSTEC STC200). Good thermal exchange between the sample and the heating block was insured using metal contact spacers. A transmission mask (VECO 0400-Copper TEM grid, pitch 63 μm, hole size 30 μm) was secured 10 μm above the sample

surface. Irradiation took place for 2 h at 40 mW/cm^2, using the circularly polarized beam from a water-cooled argon ion laser (Coherent Innova 308) tuned to 488 nm. The film surface patterns, which result from interference of edge diffraction and back-reflections, were then imaged using AFM (Asylum MFP-3D in tapping mode).

Surface Relief Gratings. Surface relief gratings were formed by securing a sample inside the heating stage and placing it adjacent to a laser-quality mirror. An expanded laser beam was used to illuminate both the sample and the mirror, such that the mirror reflection would interfere with the incident beam at the sample surface. The incident laser power was 40 mW/cm^2, and the beam was circularly polarized. Thus, the sample surface experiences an interference between right-handed and left-handed circular light, which results in the formation of a high-efficiency SRG at room temperature. The inscription angle was 20°.

Results and Discussion

Photosoftening. Figure 1 shows a surface relief grating (SRG) formed by irradiating an azo-polymer film with a sinusoidally varying light intensity pattern. This well-established surface-patterning phenomenon still lacks a satisfactory explanation, despite extensive research. In an attempt to identify the origin of this patterning, we undertook a series of atomic force microscopy measurements. The all-optical patterning of azo films can occur with high efficiency well below the material's glass-transition temperature (T_g). Polymer motion is generally completely hindered below T_g, and it therefore often suggested that patterning involves some sort of "photoplasticization" or "photosoftening" whereby the azobenzene molecular isomerization substantially decreases the elastic modulus of the host polymer network, thereby enabling a comparatively small molecular force to drive patterning. Recent literature reports of the change in modulus, measured by quartz crystal microbalance[24] and electromechanical spectroscopy,[25,26] however, show quite modest (<10%) decrease in bulk elastic modulus. We investigated this phenomenon by performing AFM force−distance measurements, which allow one to deduce the elastic properties of thin films by performing nanoindentation (a typical curve is shown in Figure 3a). By fitting the shape of many indentation and retraction curves, a range of modulus values were calculated, which is depicted as a histogram Figure 3b. From this distribution, we calculate that the average modulus of the film is 219 ± 70 kPa before irradiation, whereas it is 336 ± 62 kPa during irradiation. From both this average and the overall distribution, we conclude that there is no statistically significant difference between the two cases. Thus, consistent with the other studies, there appears not to be an orders-of-magnitude decrease in the modulus. We confirmed that we were in fact irradiating the sample volume probed by the AFM by leaving the irradiating light active for a long period of time, after which AFM topography measurements showed significant photopatterning in the vicinity of the AFM tip. It should be noted, however, that the time scale of these modulus measurements (seconds) is smaller than the typical time scale for material motion (minutes). The lack of substantial photosoftening indicates that the material motion does not involve a decrease in the bulk elastic properties of the material. Instead, it relies upon localized, molecular scale rearrangements. Evidently, the azobenzene isomerization induces a sufficient molecular pressure to distort the polymer matrix locally, rather than softening the bulk matrix substantially. This helps explain why the observed photoexpansion and surface patterning persist at room temperature: the polymer matrix is still rigid and cannot relax. These results also eliminate any model that relies upon significant photosoftening to explain mass transport.

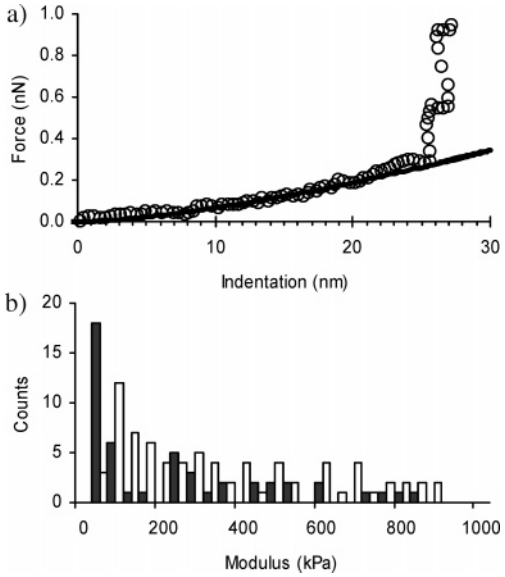

Figure 3. (a) Typical force−distance curve obtained by indenting an AFM tip into an azo-polymer thin film. The open circles are the experimental data, and the black line is a fit to the data. The sharp rise in the later part of the curve represents the "infinitely stiff" response of the sample/substrate and is not considered in the analysis. (b) Histogram of AFM modulus events, based on the fits to the force−distance data. Measurements without laser irradiation (black bars) and during irradiation with a 532 nm diode laser (white bars) are shown. The two distributions are not significantly different, indicating that photosoftening is a limited effect.

Temperature Dependence of Patterning. Our recent work using ellipsometry[18] and neutron reflectometry[19] has identified two competing photomechanical effects in azobenzene materials. Thin films of azo-polymer were irradiated homogeneously with laser light at a wavelength close the azo's absorption maximum. Below a characteristic crossover temperature, the material exhibited photoexpansion behavior, whereas above this temperature, the same material instead photocontracted. The expansion can be attributed to molecular isomerization, which induces a molecular pressure on the surrounding polymer matrix, forcing it to expand. Since the polymer matrix cannot relax at low temperature, the expansion remains fixed. At a certain temperature, however, the combination of light-induced motion and thermally enabled motion is sufficient to allow the azobenzene dipoles to reorient, aggregate, and thereby crystallize into higher-density domains. The existence of these higher-density azo domains was detected by X-ray reflectivity measurements on patterned samples[27,28] and by our neutron reflectometry measurements on homogeneously irradiated samples.[19] The temperature dependence of the photomechanical effect measured for thin films of poly(disperse red 1 acrylate) (pdr1a) is shown in Figure 2. As can be seen, a crossover from photoexpansion to photocontraction occurs at ~50 °C. The phenomenon was also found to occur in the azo-polymer poly[4′-[[2-(acryloyloxy)ethyl]ethylamino]-2-chloro-4-nitroazobenzene] (pdr13a), and it is likely that it is a generic effect that occurs in all azo materials. It should also be noted that this effect, which involves a large-scale change in material dimensions and density, occurs well below the glass-transition temperature and apparently without the aid of photosoftening.

These neutron reflectometry measurements prompted us to similarly study the temperature dependence of surface patterning in azo materials. The previous study measured expansion and contraction effects that occurred when the films were homogeneously irradiated with laser light. However, the photomechanical effect is clearly localized, as it occurs readily in thin

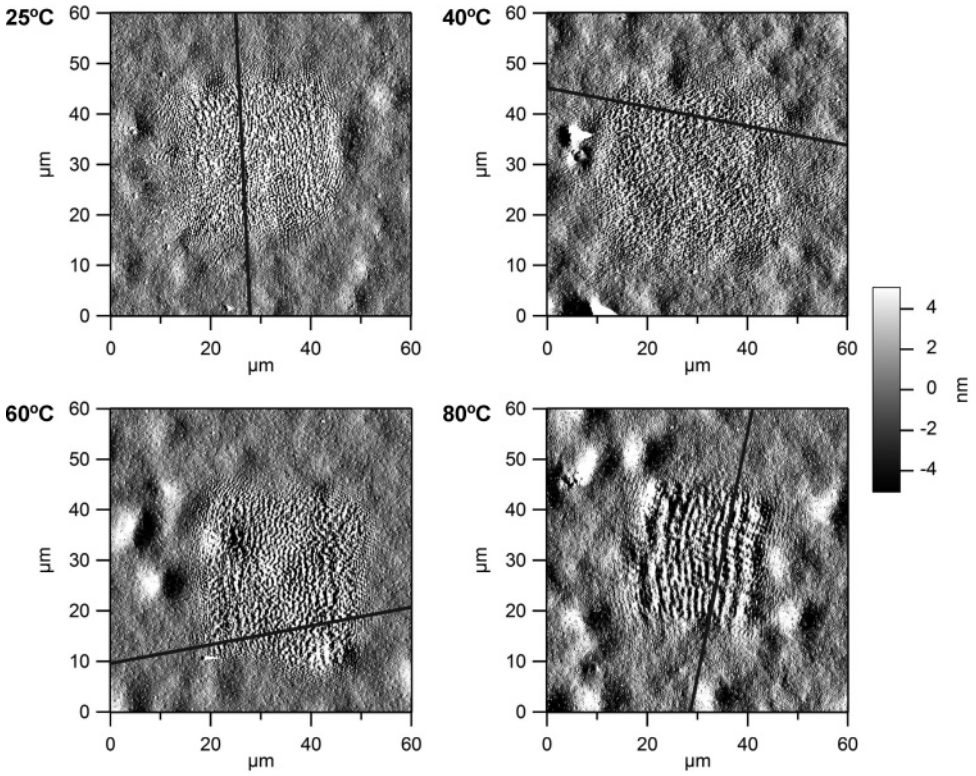

Figure 4. Atomic force microscopy amplitude images (all shown using the same vertical scale) of an azo surface irradiated through a mask with square holes. Irradiation was performed at 25, 40, 60, and 80 °C. The central region in each image is rougher because it has become photopatterned by the incident laser light. The surrounding area was not irradiated with laser light. The black line through each figure refers to the cross sections shown in Figure 5.

films even 20 nm thick. It is thus natural to consider the connection between these photomechanical motions and the surface mass transport patterning well documented in the azo system. To that end, we irradiated the same polymer material (pdr1a) through a transmission grid, so that the photomechanical transformations would be spatially localized. Figure 4 shows atomic force micrographs of the resultant changes in topography when films held at various temperatures are irradiated. In each case, the thin film was irradiated for 2 h using 40 mW/cm^2 laser light at 488 nm. The amplitude images show clearly that the irradiated region (center square in the images) has become considerably rougher than the surrounding unirradiated polymer surface. Similar photoinduced roughening[25] or spontaneous patterning[29−31] has been observed during homogeneous irradiation of related systems. It is likely due to surface patterning owing to the interference between the edge diffractions and the back-reflections from the substrate. Some amount of photoroughening may also be caused by spontaneous buckling of the sample surface to relieve the stress caused by the photomechanical deformation (whether expansion or contraction) that is occurring. Figure 5 shows the root-mean-square (rms) roughness of the corresponding height data for the irradiated regions. For comparison, the rms roughness of the unirradiated polymer surface is 15 nm. By comparing the data in Figure 2 to Figure 5, it is clear that the patterning observed by AFM follows the same temperature dependence as the photomechanical effect measured with neutron reflectometry. Specifically, the competition between the two effects causes the surface patterning to be inefficient near the crossover temperature (∼50 °C), whereas it becomes more efficient further from the crossover. The height cross sections (see Figure 6a) provide a more direct indication of nature of the surface patterning. At 25 °C, the patterning clearly involves the formation of surface relief that is higher than the surrounding polymer material. This

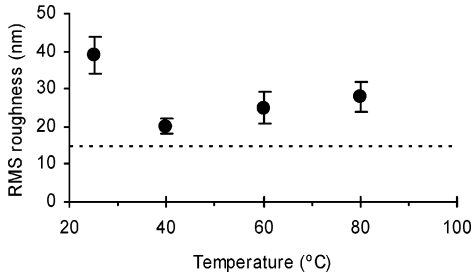

Figure 5. Root-mean-square (rms) roughness inside the patterned regions shown in Figure 3. For reference, the roughness of the surrounding (un-irradiated) film is 15 nm and is shown using a dashed line. The rms roughness can be used as a measure of patterning efficiency. The patterning is inefficient near the crossover temperature.

occurs because the irradiated film region is expanded relative to the unirradiated material. At 40 °C, the competition between the photoexpansion and photocontraction effects makes the photomechanical response quite modest, and the surface patterning is correspondingly smaller, being the result of a small amount of photoexpansion. At 60 °C, the surface patterning extends below the original film thickness. At 80 °C, the effect is even more pronounced, with the patterning phenomenon clearly arising due to contraction of the material in the irradiated region. Thus, for all temperatures a light-induced surface-patterning phenomenon is apparent. However, the phase of the patterning is opposite on either side of the crossover temperature. The patterning analysis can be made more quantitative by integrating the area under the AFM height profiles. (The curves are offset so that the unirradiated film surface corresponds to a height of zero.) The trend of this value as a function of patterning temperature (see Figure 6b), as well as the crossover temperature, closely matches the photomechanical trend observed using neutron reflectometry (Figure 2).

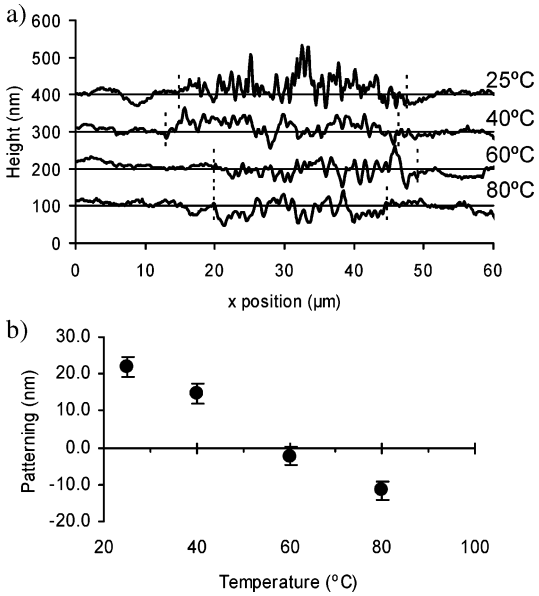

Figure 6. (a) Atomic force microscopy height cross sections, taken through the corresponding images shown in Figure 3. The sections have been offset vertically for clarity. The gray horizontal line represents the nominal film height in each case. The vertical dashed lines for each section represent the approximate boundaries of the illuminated regions, as determined from the amplitude data in Figure 3. (b) By integrating the area under the curve in the patterned region (and normalizing to the associated span), the magnitude and sign of the effect can be quantified. The patterning trend, as a function of temperature, exactly matches the photomechanical trend seen in Figure 2. The error bars are based on a similar analysis performed on the unirradiated film region.

Photomechanical Mechanism. Given the correspondence between the photomechanical data and the surface patterning data, we propose that the well-established surface mass transport phenomenon is in fact a manifestation of localized photomechanical deformation. Specifically, a light intensity gradient will generate a corresponding photomechanical stress gradient inside the azo material, which will serve to drive the motion of polymer material. Below the crossover temperature, photoexpansion in the illuminated regions will lead to a positive pressure gradient. Above the crossover temperature, photocontraction in the illuminated regions will lead to a negative pressure and a phase-inverted version of the patterning. The existence of two patterning mechanisms, one phase inverted relative to the other, has been identified in the literature. The proposed below-crossover patterning mechanism is in fact well described by the isomerization pressure mechanism[14,15] described in the literature and the related hydrodynamic modeling studies. The proposed above-crossover mechanism is essentially the same, with the inclusion of a phase-inverted stress pattern. It should also be noted that the proposed densification-based patterning, initiated by photoorientation, is similar to the mean-field model[12,13] proposed in the literature. Thus, the previously proposed isomerization pressure and mean-field models are limiting cases in the general framework of a photomechanical mechanism. It is important to note that photomechanical effects measured in azo systems, and now identified as the origin of surface patterning, occur in these materials well below T_g and without the aid of photosoftening.

In the literature, it has been found that liquid crystalline systems exhibit opposite expansion/contraction effects relative to a similar amorphous system.[16,32] This is now easily explained with the photomechanical data, with the suggestion that liquid crystalline systems are, owing to their high mobility, above their crossover temperature even at room temperature and thus exhibit photocontraction behavior. Similarly, the bending of free-standing liquid crystal films is due to photocontraction.[3] Amorphous systems, on the other hand, will typically exhibit an opposite photoexpansion behavior because they are below their crossover temperature. A similar argument can be made to explain the phase of surface relief patterning. Liquid crystalline systems have typically be seen to have the opposite phase behavior to amorphous systems. In LC systems, the material tends to accumulate in the irradiated regions, whereas in amorphous systems the material moves into the dark regions. This can be explained in the context of a pressure gradient. Although homogeneous irradiation (or large-scale irradiation, as shown in Figure 4) causes net expansion of a material below the crossover temperature, a local gradient in expansion creates a stress gradient that moves material out of the region of high stress (irradiation). The opposite behavior would be seen for a small-scale negative stress gradient in a material above the crossover temperature. Here, the contraction occurring in illuminated regions would serve to draw in more material, causing an accumulation and corresponding depletion from nearby regions. Thus, the phase-inverted patterning seen for some systems can be attributed entirely to the specific position of their crossover temperature. This enables us to also explain the rare cases where amorphous systems exhibit phase-inverted patterning[33] or where LC systems exhibit the usual patterning.[34,35] Similarly, the creation of phase-inverted surface relief gratings when irradiating with extremely high laser power[36] (>300 W/cm^2) can be attributed to localized heating, which drives the material above the crossover temperature. From modeling studies,[7] it is known that there is a modest (<5 K) change in sample temperature for most irradiation powers. At high laser power, however, one can calculate that the sample temperature will increase considerably and could be driven above the crossover temperature. Thus, the phase-inverted SRG (and thus double-period SRG) that was formed in that study is due to photoheating combined with photopatterning. It would of course be interesting to determine the relationship between the crossover temperature and the glass-transition in azopolymers. The present arguments would predict that a depressed T_g (via plasticization, lower molecular weight, etc.) would lead to a corresponding decrease in the crossover temperature.

Polarization Dependence. It is well-established that the surface-patterning phenomenon is strongly polarization dependent.[37] Both the efficiency of the process (as measured by topography height) and the exact shape of structures are affected by the incident polarization state. In essence, the topography encodes both the incident light intensity pattern and the polarization pattern. The presented photomechanical mechanism does not obviously include any polarization dependence. Presumably the extent of photomechanical response would be related only to the light intensity and not the polarization vector. However, a number of additional considerations can explain the influence of incident polarization. It has been determined that azo chromophores become photooriented by incident polarized light during surface patterning.[38−40] Azo chromophores tend to accumulate perpendicular to the incident polarization at any given position, as those chromophores that fall into these orientations will no longer be able to absorb incident photons and will therefore no longer undergo isomerization and photomotion. This orientational photodepletion can explain in some cases the low grating efficiency observed (for instance in the case of forming a SRG with two s-polarized beams) because the chromophores become photoaligned and cease to isomerize.

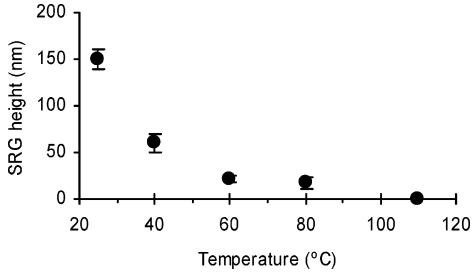

Figure 7. Surface relief grating (SRG) height, determined by AFM, for gratings patterned at a variety of temperatures (488 nm incident light, 40 mW/cm^2, mixing right-circularly polarized and left-circularly polarized beams). The grating height decreases when the patterning occurs at elevated temperatures, suggesting that this polarization combination operates using the photoexpansion mechanism.

In the context of the proposed competing photomechanical mechanism, it is also possible, however, that photoorientation increases the efficiency of the photocontraction component. For some polarization combinations this may actually increase the overall efficiency, if the photocontraction causes accumulation of material in the same direction as the photoexpansion drives material flow. Additionally, it is worth considering anisotropy in the restoring force. It is generally agreed that surface tension is the restoring force that eventually arrests the surface-patterning phenomenon. Even if the driving force is isotropic (no polarization dependence), polarization patterns may develop if the restoring force is anisotropic (has a polarization dependence). For instance, if azobenzene orientation causes the surface tension to be anisotropic (locally different along the molecular axis, as compared to against it), this can explain the observed polarization patterns. Specifically, irradiation geometries that do not induce spatial variation of the azo orientation (such as the s:s combination or the RCP:RCP combination) will have a homogeneous surface tension across the surface, which will arrest the surface mass transport. Irradiation geometries that induce a spatially varying surface tension due to a spatially varying polarization pattern and hence azo orientation (which includes the +45°:−45° and RCP:LCP combinations) will have an additional driving force to deform the sample surface, namely, that the gradient in surface tension represents an additional instability that can drive material flow. In the case of the efficient p:p combination, the polarization pattern is constant in the plane that contains the sample surface but varies in the orthogonal plane that contains the film normal.[41] As a result, the material surface will still exhibit a spatial variation of azo orientation. In these cases, the gradient in surface tension (with, importantly, lower than bulk surface tension at some positions in the pattern) will not arrest material flow as efficiently as a homogeneous surface tension. This suggestion is similar to the experimental observation of macroscopic droplet motion on azo polymer surfaces that have photodriven surface energy gradients.[42]

It is possible that further experiments measuring the temperature dependence of SRG inscription, with different polarization states, could help to determine the relative contribution of the photoexpansion and photocontraction mechanisms under each set of conditions. For instance, Figure 7 shows the SRG height for gratings formed using the highly efficient RCP:LCP polarization combination. What can be seen is that this polarization combination is inefficient at elevated temperatures, possibly because it is driven by the photoexpansion process and not efficient in a photocontraction context.

Although initial analysis of surface patterning suggested that volume was conserved,[36] subsequent studies have shown that this is not the case,[33] with evidence of densification and compressible fluid behavior. Modeling also suggests that the process requires a compressible fluid.[9] Moreover, a sequence of measurements on the thermal erasure of surface relief gratings demonstrated that during heat treatment a density grating, coincident with the initial SRG but buried beneath the surface, develops.[27,28] This suggests that the initial photopatterning and related photoorientation creates seeding crystals that can be grown, with chromophores aggregating, during thermal treatment. This is precisely analogous to the observed photomechanical effect, where the combination of light-induced orientation and heat-enabled material mobility enables a photocontracted state to be achieved.

Conclusions

AFM force−distance measurements have been used to argue that photosoftening effects are negligibly small in azo materials, which limits the range of mechanisms that can be used to explain surface patterning in these systems. The recently characterized photomechanical response of azo materials, which involves competition between photoexpansion and photocontraction, was used to explain the surface-patterning phenomenon seen in azobenzene systems. By irradiating through a gridlike mask, we have shown that surface patterning can occur both above and below the photomechanical crossover temperature. The phase of the patterning effect is opposite in the two cases, with photoexpansion driving mass transport below the crossover and photocontraction driving mass transport above the crossover temperature. This observation allows us to explain the peculiar phase dependence observed in the literature. Specifically, systems which exhibit the "common" patterning phase relationship (material motion into the dark) are constrained systems that are below their crossover temperature during patterning, whereas those that exhibit the "inverted" phase relationship (material motion into the light) are mobile systems that are above their crossover temperature.

The proposed photomechanical explanation for surface patterning agrees with the large body of literature that has been developed on azo patterning and SRG formation and does not require the introduction of a hypothetical photosoftening effect. Some of the previously proposed mechanisms can be viewed as limiting cases of this general photomechanical patterning. By including considerations of the anisotropy in the restoring force, it is also possible to explain the polarization dependence seen in azo patterning.

Acknowledgment. Neutron fitting software code was generously made available by Thad Harroun (Brock University). The neutron reflectometry data were acquired in collaboration with Helmut Fritzsche of the NRC Chalk River labs and with the help of Oleh M. Tanchak and Christopher Godbout. Polymer synthesis was performed by Nasir Ahmad. We also thank Derek Gray and Emily Cranston for help with AFM imaging and Ozzy Mermut for help with force−distance measurements. Research funds were provided by NSERC Canada and the Canadian Foundation for Innovation.

References and Notes

(1) Natansohn, A.; Rochon, P. *Chem. Rev.* **2002**, *102*, 4139.
(2) Yager, K. G.; Barrett, C. J. *J. Photochem. Photobiol. A* **2006**, *182*, 250.
(3) Yu, Y.; Nakano, M.; Ikeda, T. *Nature (London)* **2003**, *425*, 145.
(4) Camacho-Lopez, M.; Finkelmann, H.; Palffy-Muhoray, P.; Shelley, M. *Nat. Mater.* **2004**, *3*, 307.
(5) Rochon, P.; Batalla, E.; Natansohn, A. *Appl. Phys. Lett.* **1995**, *66*, 136.

(6) Kim, D. Y.; Tripathy, S. K.; Li, L.; Kumar, J. *Appl. Phys. Lett.* **1995**, *66*, 1166.
(7) Yager, K. G.; Barrett, C. J. *J. Chem. Phys.* **2004**, *120*, 1089.
(8) Kumar, J.; Li, L.; Jiang, X. L.; Kim, D. Y.; Lee, T. S.; Tripathy, S. *Appl. Phys. Lett.* **1998**, *72*, 2096.
(9) Saphiannikova, M.; Geue, T. M.; Henneberg, O.; Morawetz, K.; Pietsch, U. *J. Chem. Phys.* **2004**, *120*, 4039.
(10) Lefin, P.; Fiorini, C.; Nunzi, J. M. *Opt. Mater.* **1998**, *9*, 323.
(11) Lefin, P.; Fiorini, C.; Nunzi, J. M. *Pure Appl. Opt.* **1998**, *7*, 71.
(12) Pedersen, T. G.; Johansen, P. M. *Phys. Rev. Lett.* **1997**, *79*, 2470.
(13) Pedersen, T. G.; Johansen, P. M.; Holme, N. C. R.; Ramanujam, P. S.; Hvilsted, S. *Phys. Rev. Lett.* **1998**, *80*, 89.
(14) Barrett, C. J.; Natansohn, A. L.; Rochon, P. L. *J. Phys. Chem.* **1996**, *100*, 8836.
(15) Barrett, C. J.; Rochon, P. L.; Natansohn, A. L. *J. Chem. Phys.* **1998**, *109*, 1505.
(16) Holme, N. C. R.; Nikolova, L.; Hvilsted, S.; Rasmussen, P. H.; Berg, R. H.; Ramanujam, P. S. *Appl. Phys. Lett.* **1999**, *74*, 519.
(17) Yager, K. G.; Barrett, C. J. *Curr. Opin. Solid State Mater. Sci.* **2001**, *5*, 487.
(18) Tanchak, O. M.; Barrett, C. J. *Macromolecules* **2005**, *38*, 10566.
(19) Yager, K. G.; Tanchak, O. M.; Godbout, C.; Fritzsche, H.; Barrett, C. J. *Macromolecules*, in press.
(20) Natansohn, A.; Rochon, P.; Gosselin, J.; Xie, S. *Macromolecules* **1992**, *25*, 2268.
(21) Domke, J.; Radmacher, M. *Langmuir* **1998**, *14*, 3320.
(22) Akhremitchev, B. B.; Walker, G. C. *Langmuir* **1999**, *15*, 5630.
(23) Yager, K. G.; Tanchak, O. M.; Barrett, C. J.; Watson, M. J.; Fritzsche, H. *Rev. Sci. Instrum.* **2006**, *77*.
(24) Srikhirin, T.; Laschitsch, A.; Neher, D.; Johannsmann, D. *Appl. Phys. Lett.* **2000**, *77*, 963.
(25) Mechau, N.; Neher, D.; Borger, V.; Menzel, H.; Urayama, K. *Appl. Phys. Lett.* **2002**, *81*, 4715.
(26) Mechau, N.; Saphiannikova, M.; Neher, D. *Macromolecules* **2005**, *38*, 3894.
(27) Geue, T.; Henneberg, O.; Grenzer, J.; Pietsch, U.; Natansohn, A.; Rochon, P.; Finkelstein, K. *Colloids Surf. A* **2002**, *198*−*200*, 31.
(28) Pietsch, U.; Rochon, P.; Natansohn, A. *Adv. Mater.* **2000**, *12*, 1129.
(29) Lagugne-Labarthet, F.; Buffeteau, T.; Sourisseau, C. *Phys. Chem. Chem. Phys.* **2002**, *4*, 4020.
(30) Hubert, C.; Fiorini-Debuisschert, C.; Maurin, I.; Nunzi, J. M.; Raimond, P. *Adv. Mater.* **2002**, *14*, 729.
(31) Hubert, C.; Malcor, E.; Maurin, I.; Nunzi, J. M.; Raimond, P.; Fiorini, C. *Appl. Surf. Sci.* **2002**, *186*, 29.
(32) Bublitz, D.; Helgert, M.; Fleck, B.; Wenke, L.; Hvilsted, S.; Ramanujam, P. S. *Appl. Phys. B: Laser Opt.* **2000**, *70*, 863.
(33) Keum, C. D.; Ikawa, T.; Tsuchimori, M.; Watanabe, O. *Macromolecules* **2003**, *36*, 4916.
(34) Zettsu, N.; Fukuda, T.; Matsuda, H.; Seki, T. *Appl. Phys. Lett.* **2003**, *83*, 4960.
(35) Helgert, M.; Wenke, L.; Hvilsted, S.; Ramanujam, P. S. *Appl. Phys. B: Laser Opt.* **2001**, *72*, 429.
(36) Bian, S. P.; Williams, J. M.; Kim, D. Y.; Li, L. A.; Balasubramanian, S.; Kumar, J.; Tripathy, S. *J. Appl. Phys.* **1999**, *86*, 4498.
(37) Jiang, X. L.; Kumar, J.; Kim, D. Y.; Shivshankar, V.; Tripathy, S. K. *Appl. Phys. Lett.* **1996**, *68*, 2618.
(38) Lagugne-Labarthet, F.; Bruneel, J. L.; Buffeteau, T.; Sourisseau, C. *J. Phys. Chem. B* **2004**, *108*, 6949.
(39) Lagugne-Labarthet, F.; Bruneel, J. L.; Buffeteau, T.; Sourisseau, C.; Huber, M. R.; Zilker, S. J.; Bieringer, T. *Phys. Chem. Chem. Phys.* **2000**, *2*, 5154.
(40) Lagugne-Labarthet, F.; Bruneel, J. L.; Rodriguez, V.; Sourisseau, C. *J. Phys. Chem. B* **2004**, *108*, 1267.
(41) Viswanathan, N. K.; Balasubramanian, S.; Li, L.; Tripathy, S. K.; Kumar, J. *Jpn. J. Appl. Phys., Part 1* **1999**, *38*, 5928.
(42) Ichimura, K.; Oh, S.-K.; Nakagawa, M. *Science* **2000**, *288*, 1624.

MA061733S